Kirkwood-Dirac Nonpositivity Is a Necessary Resource for Quantum Computing

Jonathan J. Thio,[1] Songqinghao Yang,[1,2] Nicole Yunger Halpern,[3,4] Stephan De Bièvre,[5] Crispin H. W. Barnes,[1] and David R. M. Arvidsson-Shukur[2]

[1]*Cavendish Lab., Department of Physics, Univ. of Cambridge, Cambridge CB3 0HE, United Kingdom*
[2]*Hitachi Cambridge Lab., J.J. Thomson Avenue, Cambridge CB3 0HE, United Kingdom*
[3]*Joint Center for Quantum Information and Computer Science, NIST and University of Maryland, College Park, Maryland 20742, USA*
[4]*Institute for Physical Science and Technology, University of Maryland, College Park, Maryland 20742, USA*
[5]*Univ. Lille, CNRS, Inria, UMR 8524, Laboratoire Paul Painlevé, F-59000 Lille, France*

(Received 29 October 2025; revised 19 March 2026; accepted 4 June 2026; published 18 August 2026)

We elucidate the boundary between classical and quantum computation by constructing qubit Clifford circuits with nonstabilizer inputs that can be efficiently simulated classically. We do so by casting the quantum circuits realizable by defect braiding in the surface code in terms of a Kirkwood-Dirac (KD) quasiprobability distribution, a generalization of a joint probability distribution. If this distribution remains a proper (positive) probability distribution throughout a circuit, then a classical algorithm can simulate the circuit efficiently. By leveraging recent results on the geometry of KD-positive states, we construct bound-magic states. Classical computers can efficiently simulate these bound-magic states' evolutions under the circuits, although other magic states enable universal quantum computation when inputted. Furthermore, we show that KD nonpositivity is a resource monotone in this model. Thus, we establish KD nonpositivity as a necessary resource for quantum-computational advantages.

DOI: 10.1103/x819-898d

Introduction—Quantum-computing research is motivated by the expectation that quantum computers can outperform their classical counterparts. However, identifying the source of quantum advantages is notoriously difficult [1]. A deeper understanding of this issue is needed to advance quantum computing.

One may investigate the source of quantum advantages by comparing a universal model of quantum computation with a suitably restricted model. A common universal model is the quantum-computation-by-state-injection model [2]. It entails arbitrary single-qubit state preparations, Clifford gates, and computational-basis measurements. One can restrict this model by constraining its input states. If classical computers can simulate the restricted model efficiently, then (if quantum advantages exist), quantum speedups require the excluded states.

The Gottesman-Knill theorem exemplifies this approach. The theorem governs a model that includes stabilizer-state preparations (defined below), certain gates (the Clifford gates), and computational-basis measurements. Classical algorithms can simulate the Gottesman-Knill model efficiently [3,4]. Consequently, *magic* states—states that are not mixtures of stabilizer states—are necessary for quantum advantages [2]. This result implies that some magic states enable quantum advantages in the quantum-computation-by-state-injection model. One can append certain magic states, called *distillable-magic* states, to the Gottesman-Knill model. The enhanced model can efficiently simulate every quantum computation by state injection [2,5]. However, not all magic is distillable. With respect to the Gottesman-Knill model, there may exist *bound-magic* states —magic states that still yield a classically efficiently simulable model when added to the Gottesman-Knill model [6,7]. We extend the set of known classically simulable quantum circuits by constructing bound-magic states for the computational model realized by defect braiding in the surface code. Although the Gottesman-Knill model includes our model, ours becomes universal if augmented by certain distillable-magic states [8].

The main tools for identifying bound-magic states are quasiprobability distributions [7,9]. These mathematical objects resemble probability distributions but may assume (possibly nonreal) values outside [0, 1]. Consider any quasiprobability distribution of a state. If the quasiprobabilities are probabilities (lie within [0, 1]), the state is called *positive*. Classical algorithms can efficiently simulate certain quantum computations whose states are always represented by positive quasiprobability distributions

Published by the American Physical Society under the terms of the Creative Commons Attribution 4.0 International license. Further distribution of this work must maintain attribution to the author(s) and the published article's title, journal citation, and DOI.

[7,10–19]. In short, classical computers can efficiently simulate positive states. Every positive state, if not a mixture of stabilizer states, is a bound-magic state.

A prominent quasiprobability-based simulation algorithm represents odd-dimensional qudits with the Gross-Wigner function [7,20]. This quasiprobability distribution's pure positive states are the pure stabilizer states. Moreover, one can use the Gross-Wigner function to identify bound-magic states defined on odd-dimensional Hilbert spaces [21]. Since the Gross-Wigner function is defined only for odd-dimensional qudits, this construction cannot model qubit computations, the most common quantum computations [22]. References [8,15–18,23] circumvented this limitation. In particular, Ref. [8] introduced a quasiprobability distribution tailored to the operations implementable via defect braiding on the surface code. These operations act on *rebits*. A rebit is a qubit restricted to quantum states represented, relative to the computational basis, by real matrices [24]. We call this model the Delfosse-Guerin-Bian-Raussendorf (DGBR) model (Definition 1); and the associated quasiprobability distribution, the DGBR distribution. The DGBR distribution underlies an efficient classical-simulation algorithm for quantum circuits throughout which the state maintains a positive DGBR distribution [8].

In this Letter, we extend the volume of the known DGBR-positive rebit states. We do so by extending the DGBR distribution from rebits to all qubit states [Eqs. (2) and (3)]. The extended distribution, we prove, is the real part of a complex-valued Kirkwood-Dirac (KD) quasiprobability distribution [25–28] that we construct. We then show that the KD-positive states coincide with the DGBR-positive rebit states. Applying this equivalence, we characterize the rebit DGBR-positive states (Fig. 1), using a recently developed toolkit for identifying KD-positive states [29–31]. We thereby discover previously unknown bound-magic states, with respect to the DGBR model,

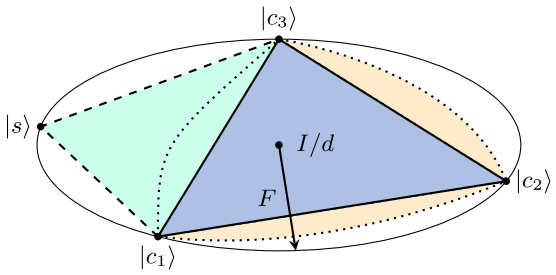


FIG. 1. Schematic overview of the efficiently classically simulable states' geometry. The disk represents the set of all two-qubit states. The boundary represents the pure states. The states $|c_j\rangle$ and $|s\rangle$ are CSS and non-CSS stabilizer states, respectively. The area bounded by the solid triangle represents the CSS polytope. The area bounded by the dashed lines represents further stabilizer mixtures. The shape enclosed by the dotted line represents the $\mathbb{Z}_2^n$-KD-positive states. The yellow region represents bound-magic states relative to the DGBR model: they are $\mathbb{Z}_2^n$-KD-positive but lie outside the stabilizer polytope.

defined on even-dimensional Hilbert spaces. That is, we identify a family of quantum circuits that is universal, given suitable magic-state inputs, but efficiently classically simulable, given our bound-magic states. Finally, we define the KD mana, a measure of our KD distribution's nonpositivity. The KD mana is an additive monotone for a resource theory of rebit quantum computation, which we define. Thus, we establish KD nonpositivity as a resource necessary for quantum-computational advantages.

Preliminaries—Consider an n-qubit system associated with the Hilbert space $\mathcal{H} = (\mathbb{C}^2)^{\otimes n}$ of dimensionality $d = 2^n$. Denote the set of density matrices on $\mathcal{H}$ by $\mathcal{D}(\mathcal{H})$. Consider representing $\rho \in \mathcal{D}(\mathcal{H})$ as a matrix relative to the computational basis. If and only if the elements are real, ρ is *real*, representing a rebit state. We index $d \times d$ matrices' elements by binary vectors $\boldsymbol{u}, \boldsymbol{v} \in \mathbb{Z}_2^n$. Furthermore, let Z_j act as the Pauli-Z operator on qubit j and as the identity everywhere else. Define X_j similarly. We denote a Pauli string associated with $\boldsymbol{u}$, $\boldsymbol{v}$ by

$$P_{\boldsymbol{u},\boldsymbol{v}} = \prod_{j=1}^{n} Z_j^{v_j} X_j^{u_j}. \tag{1}$$

This work features stabilizer states, particularly Calderbank-Shor-Steane (CSS) states, defined as follows [32–34]. The Pauli strings with phases ± 1 and $\pm i$ form the Pauli group. Consider any maximal commuting subgroup of the Pauli group. The subgroup's elements share exactly one eigenstate associated with the unit eigenvalue. The set of all such eigenstates, associated with all the maximal commuting subgroups, form the stabilizer states [1]. The CSS states are the stabilizer states whose maximal stabilizing subgroup is generated by the Z strings $P_{\boldsymbol{0},\boldsymbol{v}}$ and X strings $P_{\boldsymbol{u},\boldsymbol{0}}$. The CSS states form the logical states of the popular CSS error-correction codes [32–34].

Figure 1 summarizes properties of the aforementioned states. The convex mixtures of the stabilizer states (the *stabilizer mixtures*) form a polytope. Analogous statements govern the rebit-stabilizer states and the CSS states. The stabilizer polytope contains the rebit-stabilizer polytope, which contains the CSS polytope. Supplemental Note I [35] overviews all the states invoked in this Letter.

DGBR model and distribution—We now review an n-rebit computational model [8]. This model's gates are the gates implementable via defect braiding in surface codes [37]. Such codes underlie several experimental research programs on fault tolerance [38–40]. Let H denote the Hadamard gate; and CNOT_{ct}, the controlled-NOT gate controlled on qubit c and targeting t.

Definition 1 (DGBR model)—The DGBR model includes the following operations: (i) Initialization of qubits in CSS states. (ii) Applications of $\mathrm{H}^{\otimes n}$, CNOT_{ct}, and $P_{\boldsymbol{u},\boldsymbol{v}}$. (iii) Measurement of any qubit in the computational basis. Previous measurement outcomes may determine future operations adaptively.

By the Gottesman-Knill theorem, classical computers can efficiently simulate the DGBR model. Furthermore, classical computers can efficiently simulate a DGBR model augmented with DGBR-positive states [8]. The DGBR distribution $W:\mathcal{D}(\mathcal{H}) \to \mathbb{R}^{d\times d}$ is defined as

$$W_{\boldsymbol{u},\boldsymbol{v}}(\rho) = \mathrm{Tr}(A_{\boldsymbol{u},\boldsymbol{v}}\rho). \tag{2}$$

The distribution's phase-space point operators are

$$A_{\boldsymbol{0},\boldsymbol{0}} = \sum_{\boldsymbol{u}\cdot\boldsymbol{v}=0 \bmod 2} \frac{P_{\boldsymbol{u},\boldsymbol{v}}}{2^{2n}} \text{ and } A_{\boldsymbol{u},\boldsymbol{v}} = P_{\boldsymbol{u},\boldsymbol{v}} A_{\boldsymbol{0},\boldsymbol{0}} P^{\dagger}_{\boldsymbol{u},\boldsymbol{v}}. \tag{3}$$

A classical algorithm efficiently simulates the DGBR model enhanced by any DGBR-positive ρ_{input} [8]. The reason is that the DGBR distribution's positive pure rebit states are the CSS states, the distribution transforms covariantly under the DGBR model's unitary operations, and it satisfies a product rule with respect to tensor products.

Consider augmenting the DGBR model with the one- and two-rebit states. The augmented model is universal; it can efficiently simulate the quantum-computation-by-state-injection model and vice versa. By the quantum extended Church-Turing hypothesis [41], the augmented DGBR model therefore has the same computational power as any physical quantum computer. We may therefore study quantum computation using this model, without loss of generality.

The $\mathbb{Z}_2^n$-Kirkwood-Dirac distribution—We now extend the DGBR distribution to a KD distribution, $Q:\mathcal{D}(\mathcal{H}) \to \mathbb{C}^{d\times d}$ defined in terms of orthonormal bases $\mathcal{A}$ and $\mathcal{B}$ for $\mathcal{H}$. (Q commonly represents KD distributions; this use of the symbol does not refer to the Husimi quasiprobability function [42].) KD quasiprobability distributions [25–28] have recently been shown to have applications spanning quantum metrology [43–45], quantum foundations [30,46–52], quantum thermodynamics [53–58], and information scrambling [53,59–63].

A KD distribution's bases can be tailored to a problem. To facilitate our quantum-computational analysis, we choose for $\mathcal{A}$ to consist of the tensor products of the Pauli-Z operator's eigenstates. We define $\mathcal{B}$ analogously in terms of the Pauli-X operator. The resulting KD distribution is an instance of the general KD distribution for a finite Abelian group G [31]. This group structure underlies our results. We have chosen for G to be $\mathbb{Z}_2^n$, which leads to the aforementioned $\mathcal{A}$ and $\mathcal{B}$ choices. The group consists of elements $\boldsymbol{g} = (g_1, g_2, \ldots, g_n)$, where $g_j \in \{0, 1\}$. The group operation is addition modulo 2 ($+$). The group elements label the computational basis, $\mathcal{A} = \{|\boldsymbol{g}^{(z)}\rangle\}_{\boldsymbol{g}\in G}$. The superscript (z) denotes the Pauli-Z basis. Later, (x) denotes the Pauli-X basis. The group G has a character group $\hat{G}$. We denote also its group operation by $+.G$ and $\hat{G}$ parallel a continuous-variable system's position and momentum spaces. Momentum is a vector and a translation operator. Similarly, a character $\boldsymbol{\chi} \in \hat{G}$ is a vector $\boldsymbol{\chi} = (\chi_1, \chi_2, \ldots, \chi_n)$, where $\chi_k \in \{0, 1\}$, and a function on G: $\boldsymbol{\chi}(\boldsymbol{g}) = \prod_{j=1}^{n} (-1)^{\chi_j g_j}$. Using the characters, we define the states

$$|\boldsymbol{\chi}^{(x)}\rangle \coloneqq \frac{1}{|G|^{1/2}} \sum_{\boldsymbol{g}\in G} \boldsymbol{\chi}(\boldsymbol{g}) |\boldsymbol{g}^{(z)}\rangle. \tag{4}$$

$|G|$ denotes the number of elements in G. The second orthonormal basis is $\mathcal{B} = \{|\boldsymbol{\chi}^{(x)}\rangle\}_{\boldsymbol{\chi}\in\hat{G}}$.

With respect to this $\mathcal{A}$ and $\mathcal{B}$, a state ρ is represented by the KD distribution

$$Q_{\boldsymbol{g},\boldsymbol{\chi}}(\rho) \coloneqq \mathrm{Tr}(B_{\boldsymbol{g},\boldsymbol{\chi}}\rho). \tag{5}$$

The $\mathbb{Z}_2^n$-KD distribution has the phase-point operators

$$B_{\boldsymbol{g},\boldsymbol{\chi}} = |\boldsymbol{\chi}^{(x)}\rangle\langle\boldsymbol{\chi}^{(x)}|\boldsymbol{g}^{(z)}\rangle\langle\boldsymbol{g}^{(z)}|. \tag{6}$$

Since $\langle\boldsymbol{g}^{(z)}|\boldsymbol{\chi}^{(x)}\rangle \neq 0$, this KD distribution is informationally complete on $\mathcal{H}$ [28], unlike the DGBR distribution. Moreover, since $\langle\boldsymbol{g}^{(z)}|\boldsymbol{\chi}^{(x)}\rangle$ is real, ρ is a rebit state if and only if $Q_{\boldsymbol{g},\boldsymbol{\chi}}(\rho)$ is real. Hence, all KD-positive states are rebit states. Like ρ, measurements have KD representations [28]. Let $\{E_l\}_l$ denote a set of positive-semidefinite matrices that represents a generalized measurement [1]. The KD representation of $\{E_l\}_l$ is

$$\tilde{Q}_{\boldsymbol{g},\boldsymbol{\chi}}(E_l) = \frac{\mathrm{Tr}(B_{\boldsymbol{g},\boldsymbol{\chi}}E_l)}{|\langle\boldsymbol{g}^{(z)}|\boldsymbol{\chi}^{(x)}\rangle|^2}. \tag{7}$$

A time-evolving state's KD distribution, with a generalized measurement's KD representation, models an experiment [28,43]. The outcome probabilities follow from the overlap formula [28,31]

$$\mathrm{Tr}(E_l\rho) = \sum_{\boldsymbol{g},\boldsymbol{\chi}} \tilde{Q}_{\boldsymbol{g},\boldsymbol{\chi}}(E_l) Q_{\boldsymbol{g},\boldsymbol{\chi}}(\rho). \tag{8}$$

We now show that the $\mathbb{Z}_2^n$-KD distribution generalizes the DGBR distribution and enjoys similar simulation properties.

Theorem 1—The $\mathbb{Z}_2^n$-KD distribution has the following properties: (1) (DGBR connection) The real part of the $\mathbb{Z}_2^n$-KD distribution [64] equals the DGBR distribution:

$$\mathrm{Re}[Q_{\boldsymbol{g},\boldsymbol{\chi}}(\rho)] = W_{\boldsymbol{g},\boldsymbol{\chi}}(\rho). \tag{9}$$

(2) (Hudson's theorem) Any given pure state is $\mathbb{Z}_2^n$-KD-positive if and only if it is a CSS state. (3) (Covariance) The $\mathbb{Z}_2^n$-KD distribution is covariant with respect to the DGBR operations

$$Q_{\boldsymbol{g}_0,\boldsymbol{\chi}_0}(P_{\boldsymbol{g},\boldsymbol{\chi}}\rho P^{\dagger}_{\boldsymbol{g},\boldsymbol{\chi}}) = Q_{\boldsymbol{g}_0+\boldsymbol{g},\boldsymbol{\chi}_0+\boldsymbol{\chi}}(\rho), \tag{10}$$

$$Q_{\boldsymbol{g}\boldsymbol{\chi}}(\mathrm{H}^{\otimes n}\rho\mathrm{H}^{\otimes n\dagger}) = \overline{Q_{\boldsymbol{\chi}\boldsymbol{g}}(\rho)}, \quad \text{and} \tag{11}$$

$$Q_{\boldsymbol{g}\boldsymbol{\chi}}(\mathrm{CNOT}_{ct}\rho\mathrm{CNOT}_{ct}^{\dagger}) = Q_{A_{ct}\boldsymbol{g},B_{ct}\boldsymbol{\chi}}(\rho). \tag{12}$$

The overline denotes complex conjugation, $(A_{ct})_{jk} \coloneqq \delta_{jk} + \delta_{tj}\delta_{ck}$, and $(B_{ct})_{jk} \coloneqq \delta_{jk} + \delta_{cj}\delta_{tk}$. (4) (Products) Let $\mathcal{H}$ factorize as the tensor product $\mathcal{H} = \mathcal{H}_1 \otimes \mathcal{H}_2$. Let $\rho_1 \in \mathcal{D}(\mathcal{H}_1)$ and $\rho_2 \in \mathcal{D}(\mathcal{H}_2)$. The $\mathbb{Z}_2^n$-KD distribution factorizes as

$$Q_{(\boldsymbol{g},\boldsymbol{g}'),(\boldsymbol{\chi},\boldsymbol{\chi}')}(\rho_1 \otimes \rho_2) = Q_{\boldsymbol{g}\boldsymbol{\chi}}(\rho_1)Q_{\boldsymbol{g}'\boldsymbol{\chi}'}(\rho_2). \tag{13}$$

To prove Theorem 1-(1), we interrelate the DGBR distribution's phase-point operators [Eq. (3)] and the $\mathbb{Z}_2^n$-KD distribution's [Eq. (6)]

$$A_{\boldsymbol{g},\boldsymbol{\chi}} = \frac{1}{2}(B_{\boldsymbol{g},\boldsymbol{\chi}} + B_{\boldsymbol{g},\boldsymbol{\chi}}^{\dagger}). \tag{14}$$

Substituting Eq. (14) into Eq. (2) yields Theorem 1-(1) (Supplemental Note II [35]). By Theorem 1-(1), the DGBR-positive rebit states are the KD-positive states.

Hudson's original theorem [67] identifies the continuous-variable Wigner function's pure positive states [68]. Our Hudson theorem's proof builds on a recent result [31]. Consider the KD distributions based on any finite Abelian group G. All such distributions' pure KD-positive states have the form

$$|H;\boldsymbol{g},\boldsymbol{\chi}\rangle \coloneqq \frac{1}{|H|^{1/2}} P_{\boldsymbol{g}\boldsymbol{\chi}} \sum_{\boldsymbol{h}\in H} |\boldsymbol{h}^{(z)}\rangle. \tag{15}$$

H denotes any subgroup of G. We compute the maximal stabilizing group of the states in Eq. (15) and that of the CSS states (Supplemental Note III [35]). These groups are identical. Thus, so are the sets of states.

The covariance relation (10) follows from Eq. (29) in Ref. [31]. We prove covariance relationships (11) and (12) by evaluating the left-hand sides and using the fact that H and CNOT map eigenstates of real Pauli operators to eigenstates of real Pauli operators (Supplemental Note IV [35]). Theorem 1-(4) follows from direct calculation.

Efficient classical simulation and bound-magic states—We now identify KD-positive states that lie outside the stabilizer polytope and therefore have bound magic relative to the DGBR model (Fig. 1). Theorem 1-(1) implies that every KD-positive state is DGBR-positive. As DGBR-positive input states are efficiently classically simulable, so is the DGBR model enhanced by any $\mathbb{Z}_2^n$-KD-positive input state ρ_{input}. We rephrase the DGBR simulation algorithm in terms of KD distributions in Supplemental Note V [35].

To identify bound-magic states, we use tools for characterizing KD-positive states [29,31,69]. The single-qubit $\mathbb{Z}_2$-KD-positive states are the mixtures of $|\boldsymbol{g}^{(z)}\rangle\langle\boldsymbol{g}^{(z)}|$ and $|\boldsymbol{\chi}^{(x)}\rangle\langle\boldsymbol{\chi}^{(x)}|$ (Theorem 1.1.I of Ref. [29]). These states are the single-qubit rebit-stabilizer states. Furthermore, the DGBR algorithm can efficiently simulate only $\mathbb{Z}_2$-KD-positive states. Therefore, if the input is a tensor product of single-rebit states, the DGBR algorithm can simulate only DGBR circuits on rebit stabilizer mixtures. Thus, the $\mathbb{Z}_2^n$-KD distribution cannot identify single-qubit bound magic states within the DGBR model.

Nevertheless, the set of KD-positive states has a richer structure in higher dimensions: it may include *exotic* KD-positive mixed states that are not mixtures of KD-positive pure states [29,31]. We now show that some two-qubit KD-positive mixed states are not mixtures of stabilizer states. Informed by the bound-magic states' locations in Fig. 1, we define an operator F that is orthogonal to a facet of the CSS polytope and to a real ridge of the stabilizer polytope (which is a facet of the rebit-stabilizer polytope):

$$F = \begin{pmatrix} 1 & 0 & 1 & 1 \\ 0 & 1 & -1 & -1 \\ 1 & -1 & -1 & -2 \\ 1 & -1 & -2 & -1 \end{pmatrix}. \tag{16}$$

Using techniques from Refs. [29,31], we parametrize with $\lambda \in [-1/(-4+8\sqrt{2}), 1/(4+8\sqrt{2})]$ a state ρ_λ along the direction of F:

$$\rho_\lambda = \frac{1}{4}I + \lambda F. \tag{17}$$

Every state ρ on the CSS-and-rebit-stabilizer facet's inner side satisfies $\mathrm{Tr}(\rho F) \leq 1$. In Supplemental Note VI [35], we show that ρ_λ is KD-positive if $\lambda \in [0, 1/(4+8\sqrt{2})]$. If $\lambda > 1/20$, then $\mathrm{Tr}(F\rho_\lambda) > 1$, so ρ_λ lies outside the facet. Thus, if $\lambda \in (1/20, 1/(4+8\sqrt{2})]$, ρ_λ is a two-qubit bound-magic state relative to the DGBR model. Similar bound-magic states exist above each of the 20 facets shared by the CSS polytope and the rebit-stabilizer polytope. We prove this claim in Supplemental Note VII [35], using cdd [70], a numerical package for analyzing polytopes [71]. The code used is available from Ref. [72].

Since two-qubit bound-magic states exist, bound-magic states must exist for every number > 2 of qubits. The reason is that partially tracing over any stabilizer mixture generates another stabilizer mixture [73]. To illustrate, we denote by σ an arbitrary KD-positive single-qubit state. Let $\lambda \in (1/20, 1/(4+8\sqrt{2})]$. $\sigma^{\otimes(n-2)} \otimes \rho_\lambda$ is KD-positive by Theorem 1-(4). Moreover, $\sigma^{\otimes(n-2)} \otimes \rho_\lambda$ cannot be a stabilizer mixture: suppose it were a stabilizer mixture, and consider tracing out the first $n-2$ qubits. The result, ρ_λ, would be a stabilizer mixture [73]; but it is not, by construction. Hence bound-magic states exist for every number > 2 of qubits. A similar statement is true for exotic KD-positive states. Since the pure KD-positive states'

convex hull is the CSS polytope, and the CSS polytope is a subset of the stabilizer polytope, this also implies that exotic states exist for every number of qubits greater than 2.

Now, we quantify how much the DGBR simulation algorithm differs from the Gottesman–Knill simulation algorithm on DGBR circuits. We numerically compare the (Hilbert-Schmidt) volumes efficiently simulable by the simulation methods (Table I). Approximately 0.69% of the two-rebit states are KD-positive bound-magic states. This result increases the known set of efficiently classically simulable states by 15%. Supplemental Note VIII [35] details our sampling methodology.

We expect the bound-magic states' relative volume to vanish as $n \to \infty$. This conjecture does not prevent our algorithm from simulating reasonable DGBR models augmented with $\mathbb{Z}_2^n$-KD-positive states. In such models, one injects tensor products of k-qubit states, with k bounded by a fixed n-independent number. Allowing k to be unbounded would eliminate the need for computation, trivializing the model, as one could simply initialize the final state. Hence, our method reveals a finite relative volume of bound-magic states.

KD nonpositivity as a resource necessary for quantum advantages—Next, we bound the KD nonpositivity needed for input-enhanced DGBR models to efficiently simulate universal quantum computers. We construct a resource theory of the DGBR model with arbitrary input states. The free states are the CSS mixtures, and the free operations are those in the DGBR model. We define the *KD mana* as

$$\mathcal{M}(\rho) \coloneqq \log \sum_{g,\chi} |Q_{g,\chi}(\rho)|. \tag{18}$$

$\mathcal{M}(\rho)$ quantifies the nonpositivity in $Q_{g,\chi}(\rho)$.

Theorem 2—The KD mana has the following properties: (1) (Faithfulness) $\mathcal{M}(\rho) = 0$ if and only if ρ is KD-positive. (2) (Additivity) For all n-qubit density operators ρ and σ,

$$\mathcal{M}(\rho \otimes \sigma) = \mathcal{M}(\rho) + \mathcal{M}(\sigma). \tag{19}$$

(3) (Monotone) $\mathcal{M}$ is nonincreasing under the free operations.

TABLE I. Estimated relative volumes of the two-qubit quantum states. We estimated the relative volumes by sampling 1 billion random quantum states from the space $\mathcal{D}((\mathbb{R}^2)^{\otimes 2})$. GK stands for Gottesman-Knill.

Category	*Eff. sim. by proportion*	
Stabilizer & KD-positive	GK & DGBR	1.5614(5) %
Stabilizer & KD-nonpositive	GK	2.9753(5) %
Magic & KD-positive (bound)	DGBR	0.6868(3) %
Magic & KD-nonpositive	Neither	94.7766(6) %

Theorem 2-(1) is true because $\sum_{g,\chi} |Q_{g,\chi}(\rho)| = 1$ if and only if ρ is $\mathbb{Z}_2^n$-KD-positive [28]. Theorem 2-(2) follows from the product rule in Theorem 1-(4). We prove Theorem 2-(3) in Supplemental Note IX [35] by explicit calculation.

Using the resource theory, we can quantify the KD nonpositivity necessary for quantum computation. A DGBR model augmented by the states

$$|A\rangle = \frac{|0\rangle|0\rangle + \cos\frac{\pi}{4}|1\rangle|0\rangle + \sin\frac{\pi}{4}|0\rangle|1\rangle}{\sqrt{2}}, \text{ and} \tag{20}$$

$$|B\rangle = \frac{|0\rangle|+\rangle + |1\rangle|-\rangle}{\sqrt{2}} \tag{21}$$

can perform universal quantum computation [8]. Consider starting with m copies of a given state ρ and transforming them, via free operations, into copies of the desired state σ. We lower-bound the required m:

Corollary 1—Consider any procedure that has a nonzero probability of mapping $\rho^{\otimes m}$ to $\sigma^{\otimes n}$. The procedure requires $m > n\mathcal{M}(\sigma)/\mathcal{M}(\rho)$ copies of ρ, on average over trials.

The states $|A\rangle$ and $|B\rangle$ have nonzero KD mana [$\mathcal{M}(|A\rangle\langle A|) = 0.473$ and $\mathcal{M}(|B\rangle\langle B|) = 0.870$]. Since KD mana quantifies KD nonpositivity, we have established KD nonpositivity as a resource necessary for quantum computation.

Discussion—We have identified methods for quantifying quantum-computational advantages within the DGBR model enhanced with arbitrary input states. We generalized the rebit-restricted DGBR distribution to a $\mathbb{Z}_2^n$-KD distribution. Adapting the KD toolkit, we identified states that, when appended to the DGBR model, yield an efficiently classically simulable model. We thereby construct bound-magic states on even-dimensional Hilbert spaces. They increase by $\approx$15% the volume of the known efficiently classically simulable states.

Our construction answers and extends beyond an open question: do even-dimensional Hilbert spaces support bound-magic states? Campbell *et al.* [6] showed that standard protocols cannot distill all qubit magic states. The proof does not govern all distillation protocols, however. Furthermore, researchers had not constructed bound-magic states using the DGBR distribution (unlike the Gross-Wigner function in the context of odd-dimensional Hilbert spaces).

Our method simulates DGBR circuits with bound-magic-state inputs, although earlier methods (including Gottesman–Knill) cannot. We have thus enlarged the set of circuits known to be classically efficiently simulable. This result is independent of the DGBR model.

Last, we defined the KD mana, which quantifies the $\mathbb{Z}_2^n$-KD distribution's nonpositivity. The KD mana, we showed, is a resource monotone for DGBR computation with arbitrary input states. The KD mana provides an easy-to-calculate bound on the rate of state conversion. Our Letter

shows that KD nonpositivity is a necessary resource for quantum advantages in the DGBR model enhanced by arbitrary input states.

The $\mathbb{Z}_2^n$-KD distribution is one instance of a broader class of KD distributions [31]. Other instances simulate different computational models. The KD distribution is therefore not DGBR-specific, but a general tool for studying classical simulability. A natural next step combines our algorithm with the dynamically-updated-quasiprobability scheme of Park *et al.* [12], potentially enlarging the bound-magic set or reaching nonreal states.

Acknowledgments—J. J. T. was supported by the Cambridge Trust. The authors thank Christopher Long, Wilfred Salmon, Joe Smith, Richard Jozsa, Nicolas Delfosse, Ryuji Takagi, and Cory Aitchison for helpful discussions. This work received support from the National Science Foundation: QLCI Grant No. OMA-2120757. This work was supported in part by the Agence Nationale de la Recherche under Grant No. ANR-11-LABX0007-01 (Labex CEMPI), by the Nord-Pas de Calais Regional Council and the European Regional Development Fund through the Contrat de Projets État-Région (CPER), and by the CNRS through the MITI interdisciplinary programs.

Data availability—The data that support the findings of this article are openly available [72].

[1] M. A. Nielsen and I. L. Chuang, *Quantum Computation and Quantum Information: 10th Anniversary Edition* (Cambridge University Press, Cambridge, England, 2010).
[2] S. Bravyi and A. Kitaev, Universal quantum computation with ideal clifford gates and noisy ancillas, Phys. Rev. A **71**, 022316 (2005).
[3] D. Gottesman, The heisenberg representation of quantum computers, *Group22: Proceedings of the XXII International Colloquium on Group Theoretical Methods in Physics*, edited by S. P. Corney, R. Delbourgo, and P. D. Jarvis (International Press, Cambridge, MA, 1999), pp. 32–43.
[4] S. Aaronson and D. Gottesman, Improved simulation of stabilizer circuits, Phys. Rev. A **70**, 052328 (2004).
[5] B. W. Reichardt, Quantum universality from magic states distillation applied to CSS codes, Quantum Inf. Process. **4**, 251 (2005).
[6] E. T. Campbell and D. E. Browne, Bound states for magic state distillation in fault-tolerant quantum computation, Phys. Rev. Lett. **104**, 030503 (2010).
[7] V. Veitch, C. Ferrie, D. Gross, and J. Emerson, Negative quasi-probability as a resource for quantum computation, New J. Phys. **14**, 113011 (2012).
[8] N. Delfosse, P. Allard Guerin, J. Bian, and R. Raussendorf, Wigner function negativity and contextuality in quantum computation on rebits, Phys. Rev. X **5**, 021003 (2015).
[9] V. Veitch, S. A. Hamed Mousavian, D. Gottesman, and J. Emerson, The resource theory of stabilizer quantum computation, New J. Phys. **16**, 013009 (2014).
[10] A. Mari and J. Eisert, Positive wigner functions render classical simulation of quantum computation efficient, Phys. Rev. Lett. **109**, 230503 (2012).
[11] R. Raussendorf, D. E. Browne, N. Delfosse, C. Okay, and J. Bermejo-Vega, Contextuality and Wigner-function negativity in qubit quantum computation, Phys. Rev. A **95**, 052334 (2017).
[12] G. Park, H. Kwon, and H. Jeong, Extending classically simulatable bounds of clifford circuits with nonstabilizer states via framed Wigner functions, Phys. Rev. Lett. **133**, 220601 (2024).
[13] R. Raussendorf, J. Bermejo-Vega, E. Tyhurst, C. Okay, and M. Zurel, Phase-space-simulation method for quantum computation with magic states on qubits, Phys. Rev. A **101**, 012350 (2020).
[14] C. Okay, M. Zurel, and R. Raussendorf, On the extremal points of the lambda polytopes and classical simulation of quantum computation with magic states, Quantum Inf. Comput. **21**, 1091 (2021).
[15] M. Zurel, C. Okay, and R. Raussendorf, Hidden variable model for universal quantum computation with magic states on qubits, Phys. Rev. Lett. **125**, 260404 (2020).
[16] M. Zurel, C. Okay, and R. Raussendorf, Simulating quantum computation: How many "bits" for "it"?, PRX Quantum **5**, 030343 (2024).
[17] M. Zurel, L. Z. Cohen, and R. Raussendorf, Simulation of quantum computation with magic states via Jordan-Wigner transformations, Phys. Rev. A **112**, 042602 (2025).
[18] M. Zurel and A. Heimendahl, Efficient classical simulation of quantum computation beyond Wigner positivity, arXiv:2407.10349.
[19] H. Pashayan, J. J. Wallman, and S. D. Bartlett, Estimating outcome probabilities of quantum circuits using quasiprobabilities, Phys. Rev. Lett. **115**, 070501 (2015).
[20] D. Gross, Hudson's theorem for finite-dimensional quantum systems, J. Math. Phys. (N.Y.) **47**, 122107 (2006).
[21] There exist magic states that are positive with respect to Gross's Wigner function. Therefore, standard phase-space simulation methods can be used to simulate such states. Hence, such states must be bound-magic states.
[22] D. Schmid, H. Du, J. H. Selby, and M. F. Pusey, Uniqueness of noncontextual models for stabilizer subtheories, Phys. Rev. Lett. **129**, 120403 (2022).
[23] M. Zurel, Classical descriptions of quantum computations: Foundations of quantum computation via hidden variable models, quasiprobability representations, and classical simulation algorithms, Ph.D. thesis, University of British Columbia, 2024.
[24] T. Rudolph and L. Grover, A 2 rebit gate universal for quantum computing, arXiv:quant-ph/0210187.
[25] J. G. Kirkwood, Quantum statistics of almost classical assemblies, Phys. Rev. **44**, 31 (1933).
[26] P. A. M. Dirac, On the analogy between classical and quantum mechanics, Rev. Mod. Phys. **17**, 195 (1945).
[27] M. Lostaglio, A. Belenchia, A. Levy, S. Hernández-Gómez, N. Fabbri, and S. Gherardini, Kirkwood-Dirac quasiprobability approach to the statistics of incompatible observables, Quantum **7**, 1128 (2023).
[28] D. R. M. Arvidsson-Shukur, W. F. Braasch, Jr., S. De Bièvre, J. Dressel, A. N. Jordan, C. Langrenez, M.

Lostaglio, J. S. Lundeen, and N. Yunger Halpern, Properties and applications of the Kirkwood–Dirac distribution, New J. Phys. **26**, 121201 (2024).
[29] C. Langrenez, D. R. M. Arvidsson-Shukur, and S. De Bièvre, Characterizing the geometry of the Kirkwood–Dirac-positive states, J. Math. Phys. (N.Y.) **65**, 072201 (2024).
[30] C. Langrenez, D. R. M. Arvidsson-Shukur, and S. De Bievre, Convex roofs witnessing Kirkwood-Dirac nonpositivity, J. Phys. A **58**, 215301 (2025).
[31] S. De Bièvre, C. Langrenez, and D. Radchenko, The Kirkwood-Dirac representation associated to the fourier transform for finite abelian groups: Positivity, Ann. Henri Poincare (2025), 10.1007/s00023-025-01614-7.
[32] A. Calderbank, E. Rains, P. Shor, and N. Sloane, Quantum error correction via codes over GF(4), IEEE Trans. Inf. Theory **44**, 1369 (1998).
[33] A. Steane, Multiple-particle interference and quantum error correction, Proc. R. Soc. A **452**, 2551 (1996).
[34] D. Gottesman, Stabilizer codes and quantum error correction, arXiv:quant-ph/9705052.
[35] See Supplemental Material at http://link.aps.org/supplemental/10.1103/x819-898d for detailed proofs, which includes Ref. [36].
[36] K. Zyczkowski and H.-J. Sommers, Induced measures in the space of mixed quantum states, J. Phys. A **34**, 7111 (2001).
[37] R. Raussendorf and J. Harrington, Fault-tolerant quantum computation with high threshold in two dimensions, Phys. Rev. Lett. **98**, 190504 (2007).
[38] S. Krinner, N. Lacroix, A. Remm, A. Di Paolo, E. Genois, C. Leroux, C. Hellings, S. Lazar, F. Swiadek, J. Herrmann, G. J. Norris, C. K. Andersen, M. Müller, A. Blais, C. Eichler, and A. Wallraff, Realizing repeated quantum error correction in a distance-three surface code, Nature (London) **605**, 669 (2022).
[39] C. K. Andersen, A. Remm, S. Lazar, S. Krinner, N. Lacroix, G. J. Norris, M. Gabureac, C. Eichler, and A. Wallraff, Repeated quantum error detection in a surface code, Nat. Phys. **16**, 875 (2020).
[40] Google Quantum AI and Collaborators, Quantum error correction below the surface code threshold, Nature (London) **638**, 920 (2025).
[41] E. Bernstein and U. Vazirani, Quantum complexity theory, SIAM J. Comput. **26**, 1411 (1997).
[42] K. Husimi, Some formal properties of the density matrix, Proc. Phys. Math. Soc. Jpn. 3rd Ser. **22**, 264 (1940).
[43] D. R. M. Arvidsson-Shukur, N. Yunger Halpern, H. V. Lepage, A. A. Lasek, C. H. W. Barnes, and S. Lloyd, Quantum advantage in postselected metrology, Nat. Commun. **11**, 3775 (2020).
[44] N. Lupu-Gladstein, Y. B. Yilmaz, D. R. M. Arvidsson-Shukur, A. Brodutch, Arthur O. Pang, A. M. Steinberg, and N. Yunger Halpern, Negative quasiprobabilities enhance phase estimation in quantum-optics experiment, Phys. Rev. Lett. **128**, 220504 (2022).
[45] J. H. Jenne and D. R. M. Arvidsson-Shukur, Unbounded and lossless compression of multiparameter quantum information, Phys. Rev. A **106**, 042404 (2022).
[46] Y. Aharonov, D. Z. Albert, and L. Vaidman, How the result of a measurement of a component of the spin of a spin-1/2 particle can turn out to be 100, Phys. Rev. Lett. **60**, 1351 (1988).
[47] J. Dressel, M. Malik, F. M. Miatto, A. N. Jordan, and R. W. Boyd, Colloquium: Understanding quantum weak values: Basics and applications, Rev. Mod. Phys. **86**, 307 (2014).
[48] S. Pang, J. Dressel, and T. A. Brun, Entanglement-assisted weak value amplification, Phys. Rev. Lett. **113**, 030401 (2014).
[49] M. F. Pusey, Anomalous weak values are proofs of contextuality, Phys. Rev. Lett. **113**, 200401 (2014).
[50] J. Dressel, Weak values as interference phenomena, Phys. Rev. A **91**, 032116 (2015).
[51] S. Pang and T. A. Brun, Improving the precision of weak measurements by postselection measurement, Phys. Rev. Lett. **115**, 120401 (2015).
[52] J. J. Thio, W. Salmon, Crispin H. W. Barnes, S. De Bièvre, and D. R. M. Arvidsson-Shukur, Verification of contextuality by noncontextual experiments, Phys. Rev. A **112**, 062230 (2025).
[53] N. Yunger Halpern, Jarzynski-like equality for the out-of-time-ordered correlator, Phys. Rev. A **95**, 012120 (2017).
[54] M. Lostaglio, Quantum fluctuation theorems, contextuality, and work quasiprobabilities, Phys. Rev. Lett. **120**, 040602 (2018).
[55] M. Lostaglio, Certifying quantum signatures in thermodynamics and metrology via contextuality of quantum linear response, Phys. Rev. Lett. **125**, 230603 (2020).
[56] A. Levy and M. Lostaglio, Quasiprobability distribution for heat fluctuations in the quantum regime, PRX Quantum **1**, 010309 (2020).
[57] M. Lostaglio, A. Belenchia, A. Levy, S. Hernández-Gómez, N. Fabbri, and S. Gherardini, Kirkwood-Dirac quasiprobability approach to the statistics of incompatible observables, Quantum **7**, 1128 (2023).
[58] T. Upadhyaya, W. F. Braasch, G. T. Landi, and N. Yunger Halpern, Non-Abelian transport distinguishes three usually equivalent notions of entropy production, PRX Quantum **5**, 030355 (2024).
[59] N. Yunger Halpern, B. Swingle, and J. Dressel, Quasiprobability behind the out-of-time-ordered correlator, Phys. Rev. A **97**, 042105 (2018).
[60] R. Mohseninia, J. R. G. Alonso, and J. Dressel, Optimizing measurement strengths for qubit quasiprobabilities behind out-of-time-ordered correlators, Phys. Rev. A **100**, 062336 (2019).
[61] J. R. González Alonso, N. Yunger Halpern, and J. Dressel, Out-of-time-ordered-correlator quasiprobabilities robustly witness scrambling, Phys. Rev. Lett. **122**, 040404 (2019).
[62] N. Yunger Halpern, A. Bartolotta, and J. Pollack, Entropic uncertainty relations for quantum information scrambling, Commun. Phys. **2**, 92 (2019).
[63] S. Gherardini and G. De Chiara, Quasiprobabilities in quantum thermodynamics and many-body systems, PRX Quantum **5**, 030201 (2024).
[64] The real part of a KD distribution is sometimes called a Terletsky-Margenau-Hill distribution [65,66].

[65] H. Margenau and R. N. Hill, Correlation between measurements in quantum theory, Prog. Theor. Phys. **26**, 722 (1961).
[66] Y. P. Terletsky, On the classical limit of quantum mechanics, Zh. Eksp. Teor. Fiz. **1290** (1937).
[67] R. Hudson, When is the Wigner quasi-probability density non-negative?, Rep. Math. Phys. **6**, 249 (1974).
[68] E. Wigner, On the quantum correction for thermodynamic equilibrium, Phys. Rev. **40**, 749 (1932).
[69] C. Langrenez, W. Salmon, S. De Bièvre, J. J. Thio, C. K. Long, and D. R. M. Arvidsson-Shukur, The set of Kirkwood-Dirac positive states is almost always minimal, Phys. Rev. A **113**, 062215 (2026).
[70] K. Fukuda, cdd/cdd+ Reference Manual, ETH Zurich (1995), available at https://github.com/cddlib/cddlib.
[71] Certain software is identified in this paper to specify the experimental procedure adequately. Such identification is not intended to imply recommendation or endorsement of any product or service by NIST; nor is it intended to imply that the software identified is necessarily the best available for the purpose.
[72] J. J. Thio, KDQuantumComputation, https://github.com/JJThi0/KDQuantumComputation (2025).
[73] K. M. R. Audenaert and M. B. Plenio, Entanglement on mixed stabilizer states: Normal forms and reduction procedures, New J. Phys. **7**, 170 (2005).